Unprecedented Enhancement and Preservation of Cytochrome-C Peroxidase activity Packaged with Ionic Liquid-Modified Gold Nanoparticles by offsetting Temperature and Time Stresses

Sumit Kumar, Anamika Sindhu and Pannuru Venkatesu*

Department of Chemistry, University of Delhi, Delhi 110 007, India

Experimental techniques

Transmission electron microscopy (tem) measurement

TECHNAI 200 kV TEM (Fei, Electron optics) instrument installed at SAIF, AIIMS has been used for size, morphology and shape determination of IL modified AuNP. Samples were loaded on the 200 square mesh copper grids coated with carbon layer. Grids were washed with water with tilting and pouring around the edges. Final sample loaded copper grids were with gross humidity of < 2 % have been used for final TEM measurements.

Activity determination of Cyt-c

Peroxidase activity of Cyt c activity was determined considering ABTS as a substrate in the presence of H_2O_2. This is being due to oxidation of ABTS substrate by Cyt c which produce green colored ABTS+ radical and initiated H_2O_2. The final change in the concentration of radial is measured by UV spectroscopy at wavelength 420 nm for five minutes. Cyt c concentration (0.124 mg/mL) was mixed with ABTS (3 mM), and thereafter H_2O_2 was added (1 mM) while keeping the 2, 4 and 6 nM concentration of IL mediated AuNPs. For long term preservation study, complete protocol has been repeated after 15, 30 and 45 days. Moreover, the effect of temperature on the activity of Cyt-C in the presence of IL mediated AuNPs has also been determined at 30, 45, 60, 75 and 90 °C. Finally, the concentration of radical (ABTS+•) was calculated with Beer–Lambert Law ($ABTS^{+}$• at λ_{415} nm (ε_{415}=3.6 × 104 $M^{-1}cm^{-1}$). Herein, activity of Cyt-c is being defined as amount of radical which is being produced by 1 μmol of cyt per min.

Dynamic light scattering and zeta potential measurement

Hydrodynamic diameter (dH) and zeta-potential of Cyt-c has been calculated using a Malvern instrument, model no. Zetasizer Nano ZS90. Model is operating at λ=633 nm using He-Ne laser lamp of 4 mW, vertically emitting polarized light at reflecting angle of 90°. For considering the average value, set of 3 measurements has been taken per sample. The measurement is depending

upon on Stokes−Einstein equation which relate the speed of particles with their size under different Brownian motion. All available data are analyzed using the Malvern Zetasizer Software version 7.01. For both the DLS measurements and Zeta-potential, all samples are prepared by adding 0.5 mg/mL of Cyt-c enzymes in increasing concentration (2, 6 and nM) naked AuNPs and IL-modified AuNPs. Zeta-potential measurement was carried out using DTS1070 disposable cuvettes.

Fourier transmission infrared measurement

Thermo scientific Nicolet iS50 FT-IR spectrometer has been used to carry out to amide I and amide II interactions. Sample was measured by forming a thin film of 10 µL between the ZnSe windows and teflon spacers. D_2O was used to prepare the D_2O buffer and diminish the effect of water.

UV- Visible absorption spectra analysis

All UV-visible spectra of Cyt-c are obtained by a double beam UV-visible spectrophotometer (UV-1800), Shimadzu Co., Japan, having wavelength accuracy of ±0.3 nm and spectral bandwidth of 1.0 nm. All spectra were recorded in range of 200- 700 nm at room temperature. All spectra of Cyt-c and IL mediated AuNPs have been obtained with considering the average of three scans.

Steady-State intrinsic fluorescence analysis

Cary Eclipse spectro-fluorimeter (Varian optical spectroscopy instruments, Mulgrave, Australia) has been used for intrinsic fluorescence calculation of Cyt-c in pure state and in the presence of IL-mediated AuNPs. Spectrofluorimeter is also equipped with temperature controlling peltier system to monitor the temperature. Moreover, the excitation wavelength is set at 295 nm in the emission spectra of the instrument.

Circular Dichroism (CD) Spectroscopy Analysis

JASCO-185, CD spectrophotometer (Applied Photophysics, U.K.) equipped with chiller for temperature controller have been used for secondary structure and tertiary structure of Cyt-c. Circular dichroism (CD) spectroscopic studies are being performed using, equipped with peltier system for the controlling of temperature and having an accuracy of ±0.1 ^{o}C. Similarly, to determine the denaturing temperature of Cyt-c in pure state and in the presence of IL-mediated

AuNPs, sharp change in CD molar ellipticity was observed at λ_{222}. Secondary structure variation can also be analysed by dichroweb software.

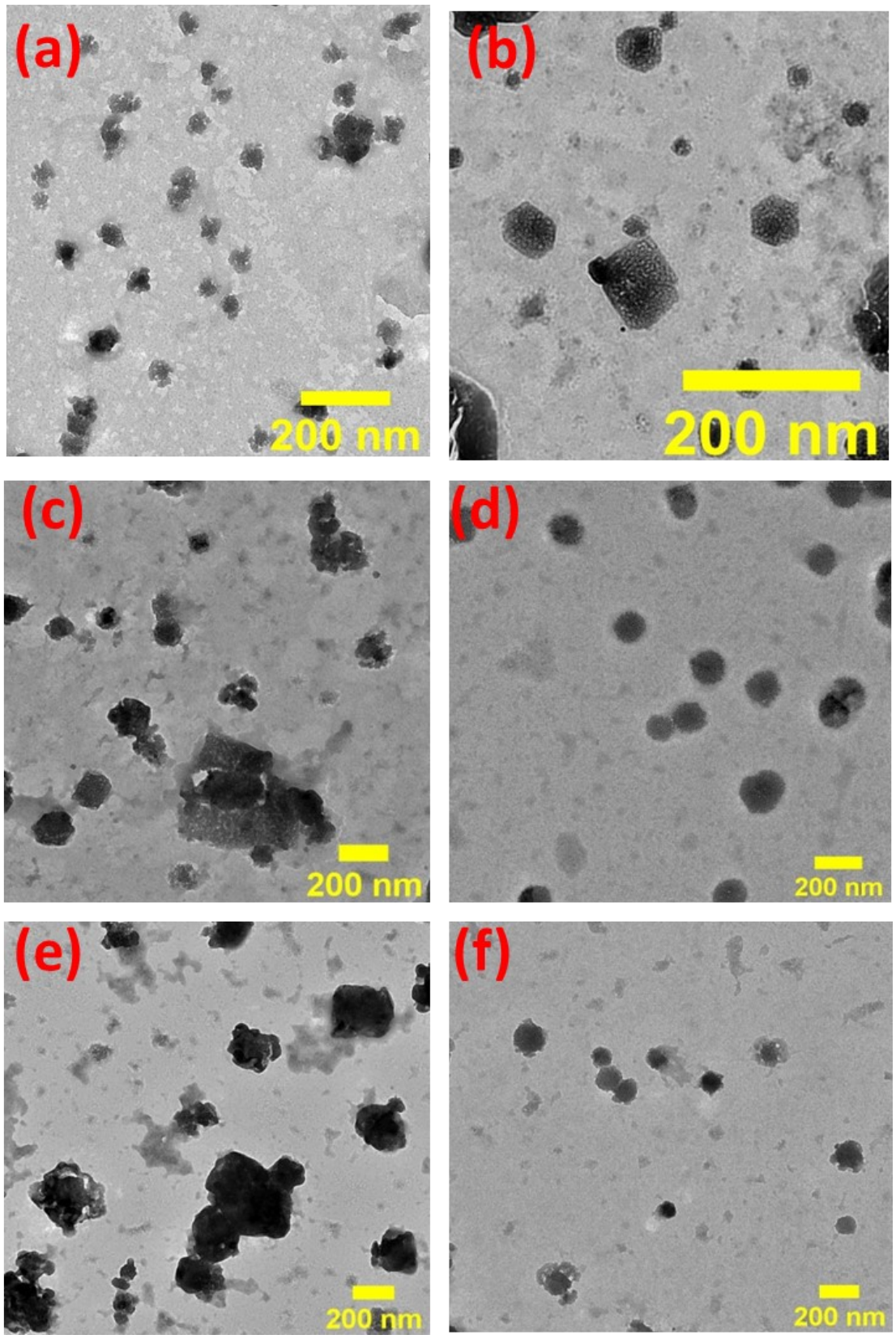
(a)
200 nm
(b)
200 nm
(c)
200 nm
(d)
200 nm
(e)
200 nm
(f)
200 nm

Figure S1. Additional TEM images of Cyt-c with AuNP-ILs. The morphology and size have been determined with Transmission electron microscope (TEM) using a scale 200 nm of Cyt-c in pure state and in the presence of IL-mediated AuNPs. The corona formation of pure Cyt-c has been represented in (a) buffer, (b) naked AuNP (c) AuNP-IL1, (d) AuNP-IL2, (e) AuNP-IL3 and (f) AuNP-IL4.

Variation of Zeta-potential on interaction of Cyt-c with AuNP-IL

The result from Figure 5 proves that incubation of Cyt-c in the lower concentration (2 nM) of naked AuNP, AuNP-IL2 and AuNP-IL4 has negative Zeta potential, and magnitude is having order of naked AuNP < AuNP-IL2 < AuNP-IL4. The incubation of Cyt-c in the lower concentration of AuNP-IL1 and AuNP-IL3, results in positive Zeta potential value of Cyt-c-AuNP-IL1 system, whereas the Zeta potential value of Cyt-c-AuNP-IL3 remains meager. Furthermore, the incubation of Cyt-c in the higher concentration of all AuNPs has increased the magnitude of Zeta potential positively and order of Zeta potential values come out to be AuNP-IL2 ~ AuNP-IL3 > AuNP-IL4 > AuNP-IL1 > Naked AuNP. The incubation of Cyt-c in higher concentration (10 nM) of all AuNPs has reshuffled the order and it comes out to be AuNP-IL3 > AuNP-IL4 > AuNP-IL2 > AuNP-IL1 > Naked AuNP.

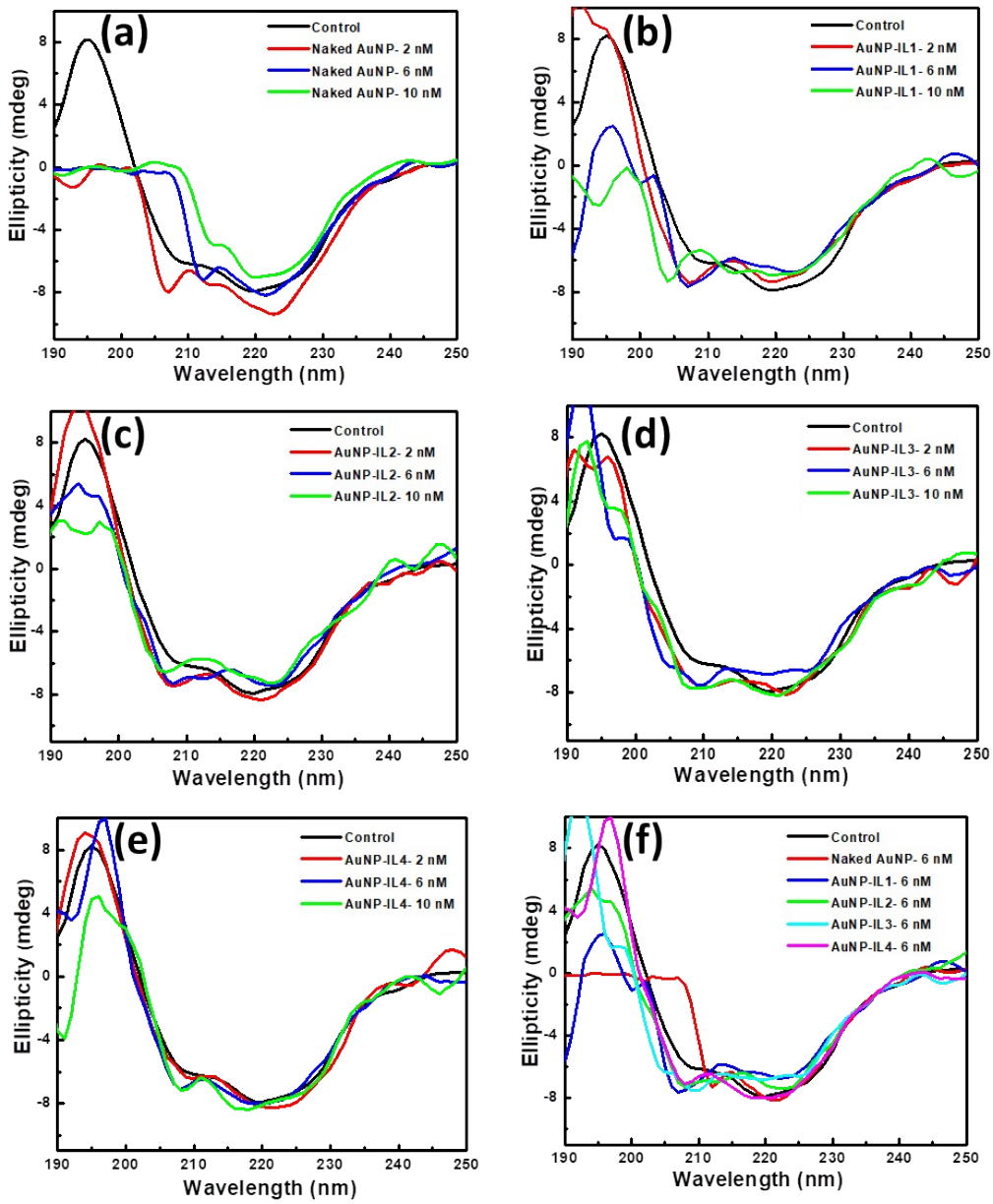

Figure S2. The secondary structure analysis of control (Cyt-c in black) has been represented in the presence of various concentrations of (a) naked AuNP, (b) AuNP-IL1, (c) AuNP-IL2, (d) AuNP-IL3, and (e) AuNP-IL4. Moreover, in Figure f, the variation in the secondary structure of control has been compared in the presence of all IL-mediated AuNPs at concentration 6 nM.

Thermal CD Analysis of the Cyt-c in the Presence of Various Concentrations of IL-Modified AuNPs

The thermal denaturation of Cyt-c has been monitored with far-UV CD in the presence of various concentrations of IL-modified AuNPs in Figures S3, S4 and S5. The ellipticity values at 222 nm have been plotted against temperature in Figure 7 to determine the thermal denaturation behavior of Cyt-c in the presence of all AuNPs. At lower concentration and lower temperature, most of the curve shows the helical pattern. The change in the secondary structure of Cyt-c in the presence of lower concentration of all AuNPs has been represented in Figure S3. Afterward, to summarize the thermal denaturation results of lower concentration (2 nM), the ellipticity values at 222 nm has been plotted against temperature in Figure 7. The combining results of Figures 3 and 6 have confirmed that the denaturation temperature (T_m) of pure Cyt-c is ~ 85 ºC which is in accordance to the literature.[34] In the middle concentration (6 nM) of all AuNPs, more rigorous changes in the thermal stability of the Cyt-c have been observed which can be analyzed from Figures S4 and 7. For Cyt-c in naked AuNP, the band at 208 has been lost completely with increase in the temperature which can be seen in Figure S4 (a) and thus confirmed the decrease in the T_m value form Figure 7 (a). Similar results of less thermal stability have been observed from Figures S4 (b) and 7 (b) in the presence of middle concentration of AuNP-IL1.

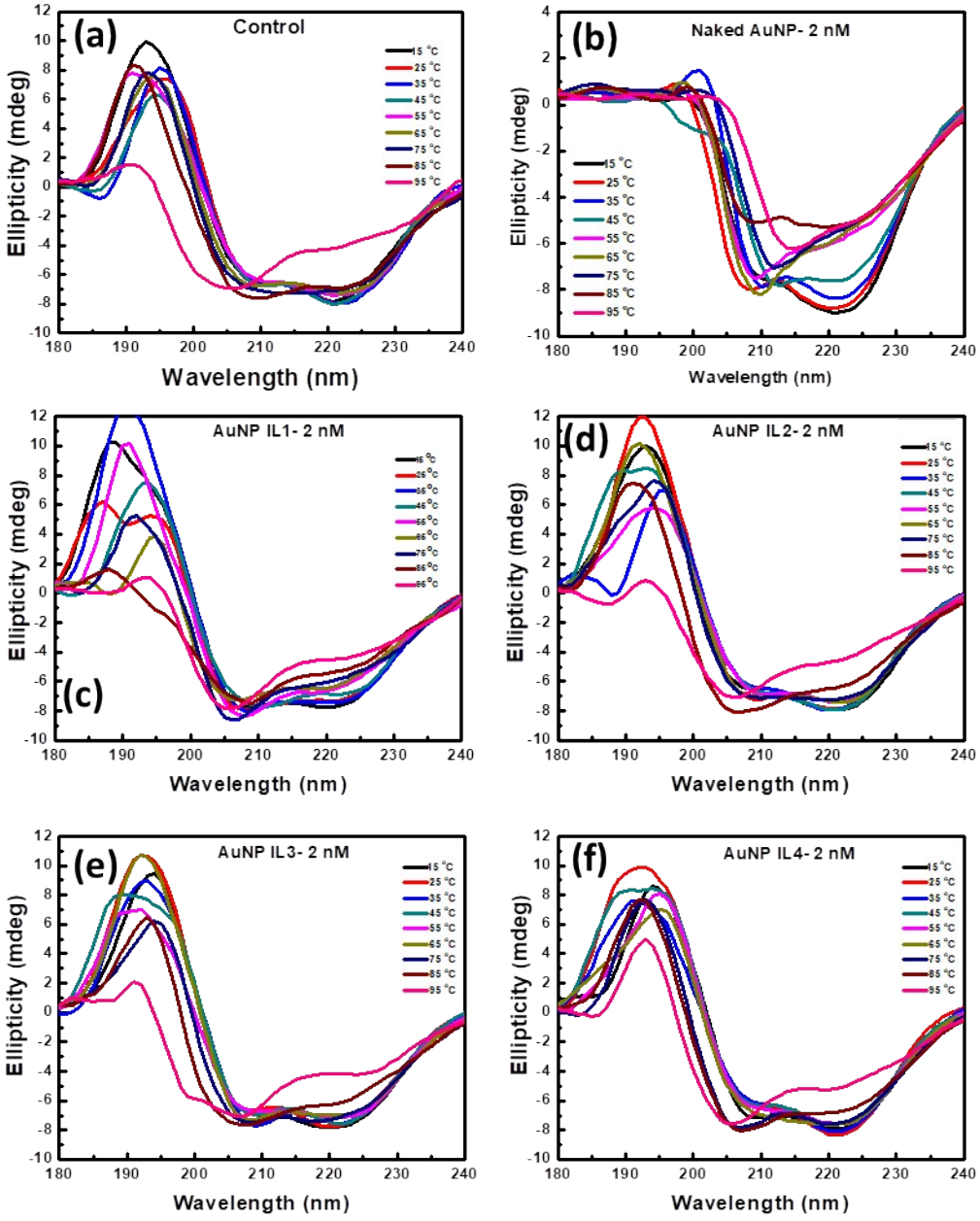

Figure S3. The temperature-induced changes in the secondary structure of Cyt-c have been represented in the presence of (a) control and in the presence of (b) naked AuNP, (c) AuNP-IL1, (d) AuNP-IL2, (e) AuNP-IL3, and (f) AuNP-IL4 with keeping the concentration of all AuNPs at 2 nM as a function of temperature.

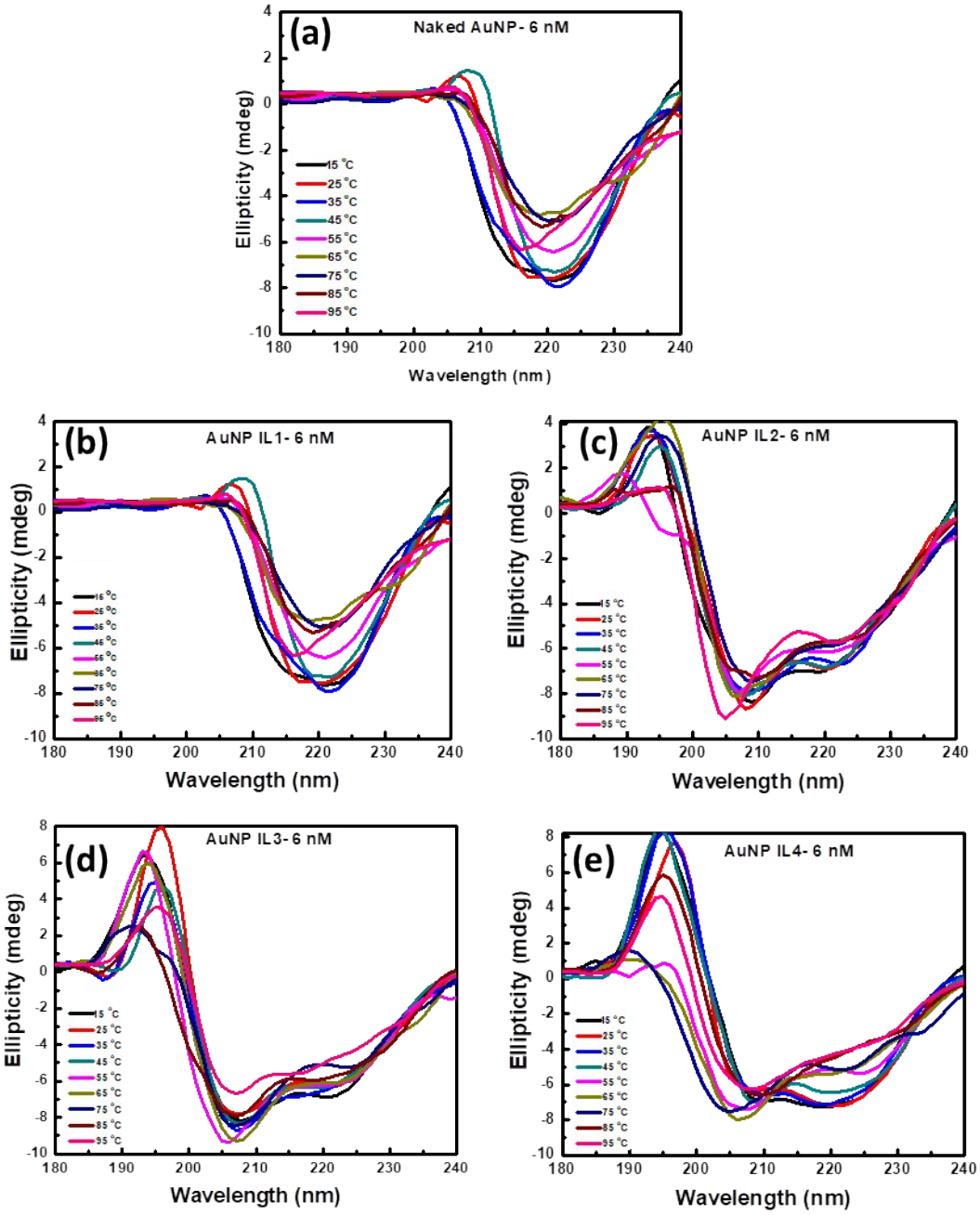

Figure S4. The temperature-induced changes in the secondary structure of Cyt-c have been represented in the presence of (a) naked AuNP, (b) AuNP-IL1, (c) AuNP-IL2, (d) AuNP-IL3, and (e) AuNP-IL4 with keeping the concentration of all AuNPs at 6 nM as a function of temperature.

The thermal denaturation data of Cyt-c of all IL-modified AuNPs at 10 nM have been provided in Figure S5. Herein, from Figure S5 (a) the lost in the 208 peaks of Cyt-c has been observed again at higher concentration of the naked AuNP. Moreover, the 222 ellipticity data from Figure 7 (a) has confirmed the more denaturation of the Cyt-c with increase in the concentration of the naked AuNPs. Furthermore, the results from Figures S5 (b) and S5 (c) have shown that the denaturation of Cyt-c in the presence of higher concentration of AuNP-IL1 and AuNP-IL2, respectively.

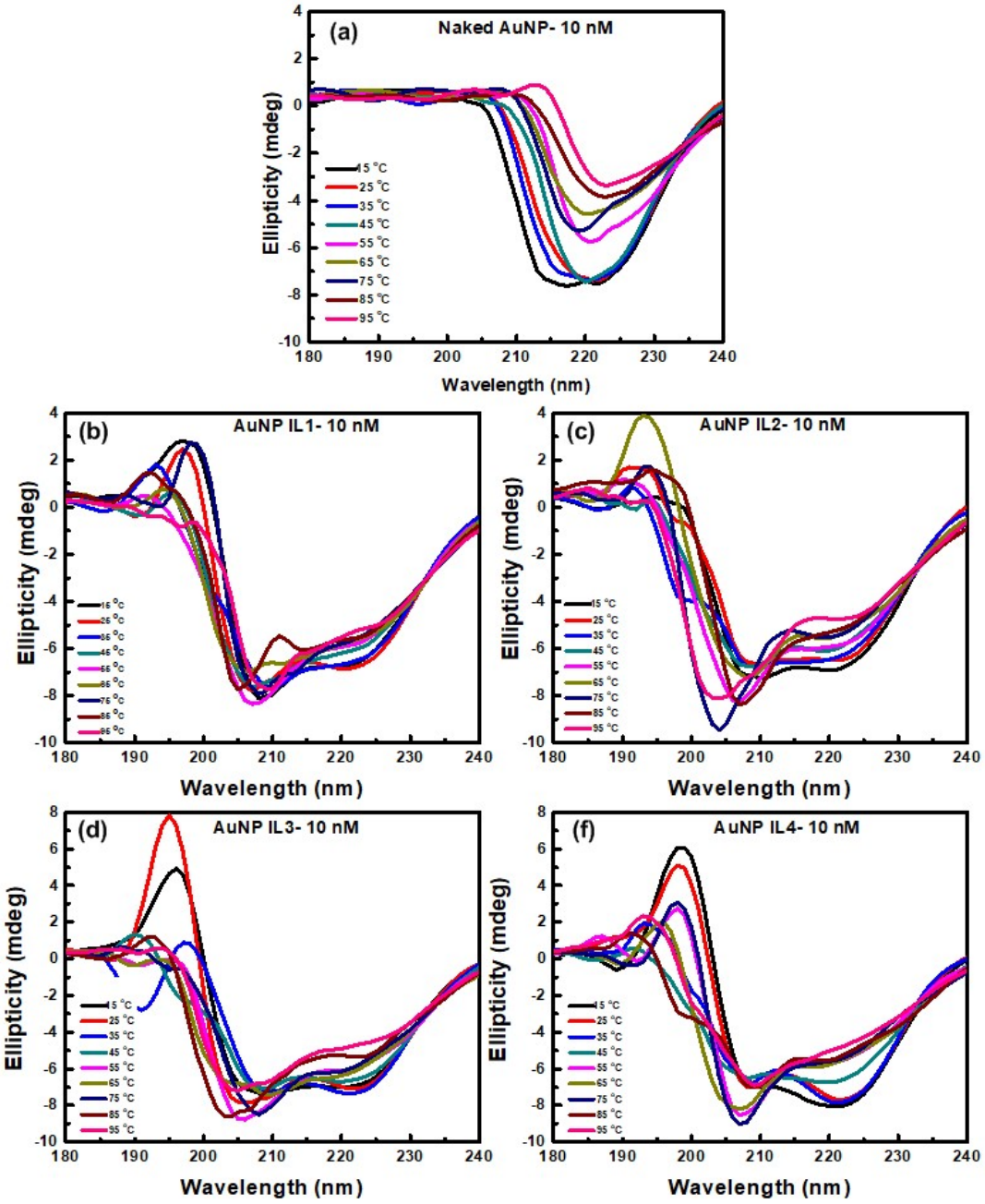

Figure S5. The temperature-induced changes in the secondary structure of Cyt-c have been represented in the presence of (a) naked AuNP, (b) AuNP-IL1, (c) AuNP-IL2, (d) AuNP-IL3, and (e) AuNP-IL4 with keeping the concentration of all AuNPs at 10 nM as a function of temperature.

Temperature-Induced Secondary Structural Composition Changes of Cyt-c in the Various Concentrations of IL-modified AuNPs using Dichroweb

The temperature affected the secondary structure compositions of the pure Cyt-c as can be seen in Figure S6 (a). It can be observed that with increase in the temperature of the system, the α-helix has been affected greatly and more compositions of the β-turn and unordered structure have been observed on the expense of α-helix and β-strand. Moreover, the effect of temperature increase on the Cyt-c incubated with naked AuNPs has been represented in Figures S6 (b), (c) and (d) for various concentrations of 2, 6 and 10 nM, respectively. The secondary structure compositional data of Cyt-c in the presence of naked AuNP has confirmed that with increased in the concentration from 2 nM to higher; the more β-strand structure can be confirmed on the expenses of the α-helix. Therefore, the higher concentration of naked AuNP is not suitable to preserve the secondary structure of the Cyt-c against temperature gradient. Consecutively, the effect of temperature increase on the Cyt-c incubated with AuNP-IL1 has been represented in Figures S7 (a), (b) and (c) for various concentrations of 2, 6 and 10 nM, respectively. The less increase in the unordered structure has been observed at lower concentrations with increase in the temperature, whereas at higher concentrations of AuNP-IL1 the more enhancements in the unordered structures have been observed at the expense of α-helix and β-strand.

Moreover, the effect of temperature increase on the Cyt-c incubated with AuNP-IL2 has been represented in Figures S8 (a), (b) and (c) for various concentrations of 2, 6 and 10 nM, respectively. At a lower concentration of AuNP-IL2, more enhancements in the β-turn and unordered structure are observed while the α-helix and β-strand compositions decrease. At a higher concentration of AuNP-IL2, the more increase in the unordered structure has been observed while β-strand compositions decrease with temperature.

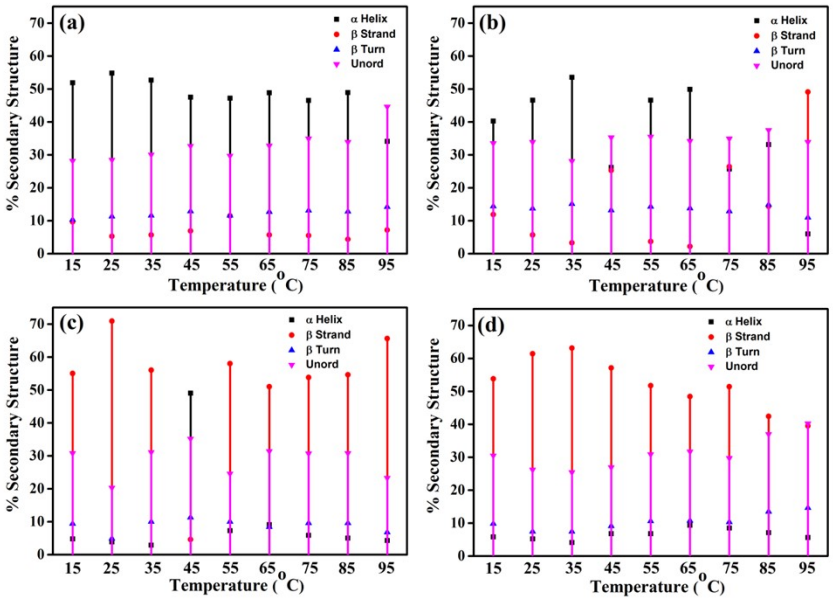

Figure S6. The assessment of secondary structure components of the Cyt-c in the presence of (a) buffer and in the presence of naked AuNP with concentration (b) 2 nM, (c) 6 nM, and (d) 10 nM against temperature gradient from 15 to 95 ºC using dichroweb software.

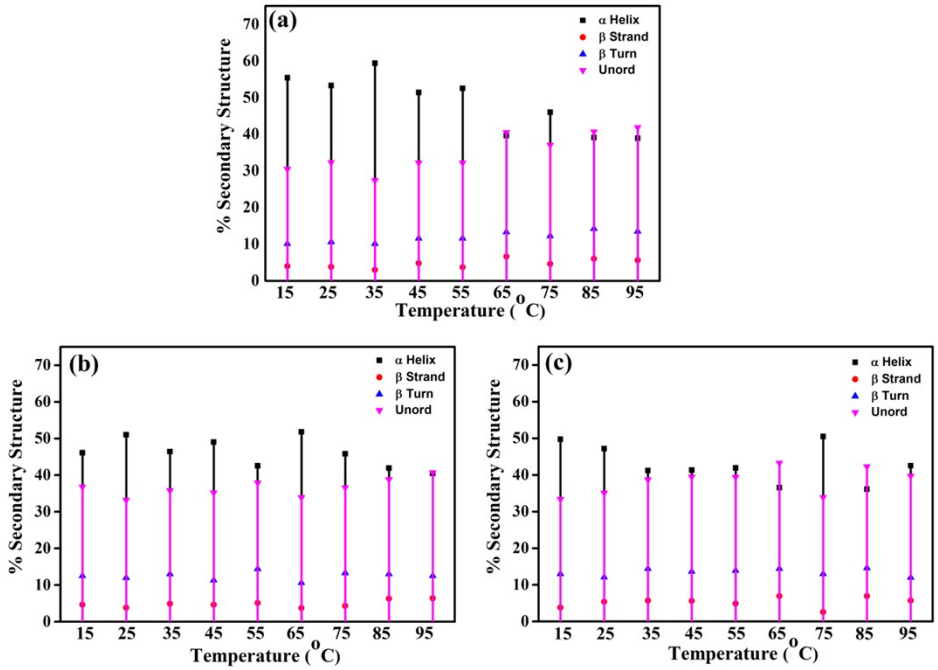

Figure S7. The assessment of secondary structure components of the Cyt-c in the presence AuNP-IL1 with concentration (a) 2 nM, (b) 6 nM, and (c) 10 nM against temperature gradient from 15 to 95 ºC using dichroweb software.

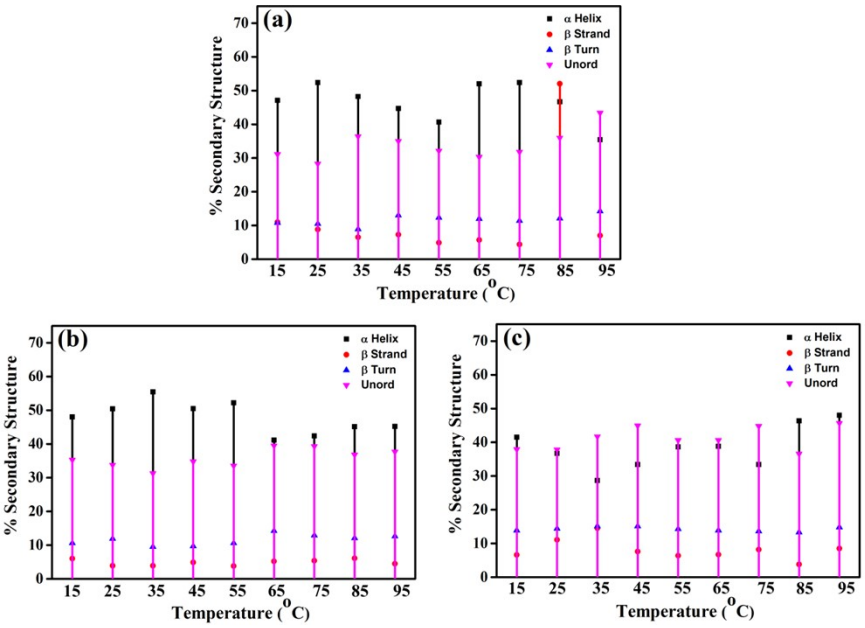

Figure S8. The assessment of secondary structure components of the Cyt-c in the presence AuNP-IL2 with concentration (a) 2 nM, (b) 6 nM, and (c) 10 nM against temperature gradient from 15 to 95 ºC using dichroweb software.

The influence of temperature increase on the Cyt-c incubated with AuNP-IL3 has been illustrated in Figures S9 (a), (b) and (c) for various concentrations of 2, 6 and 10 nM, respectively. At lower concentration of AuNP-IL3, the α-helix structure of the Cyt-c has been decreased with the increase in the temperature whereas more enhancements in the β-turn and unordered structure have been observed. Furthermore, at a higher concentration of AuNP-IL3, more decrement in β-strand has been observed with an increase in the temperature.

Finally, the effect of temperature on the Cyt-c incubated with AuNP-IL4 has been shown in Figures S10 (a), (b) and (c) at different concentrations of 2, 6 and 10 nM, respectively. At a lower concentration of AuNP-IL4, more enhancements in the unordered structure are observed while the α-helix and β-strand compositions decrease further with increase in the temperature. However, at higher concentration of AuNP-IL4, more increase in the β-turn has been observed while β-strand compositions decrease with temperature.

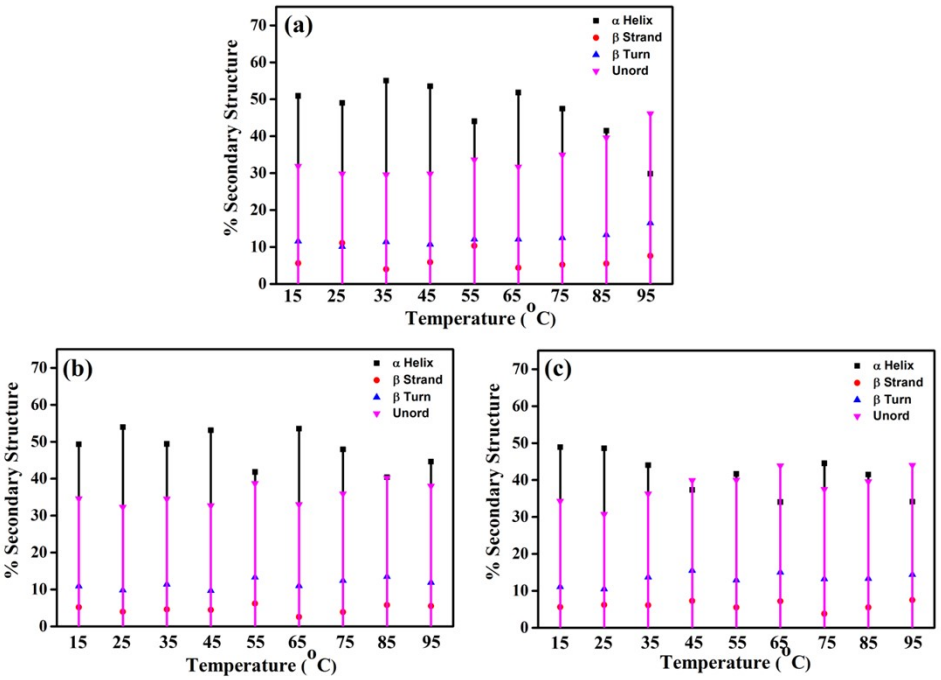

Figure S9. The assessment of secondary structure components of the Cyt-c in the presence AuNP-IL3 with concentration (a) 2 nM, (b) 6 nM, and (c) 10 nM against temperature gradient from 15 to 95 ºC using dichroweb software.

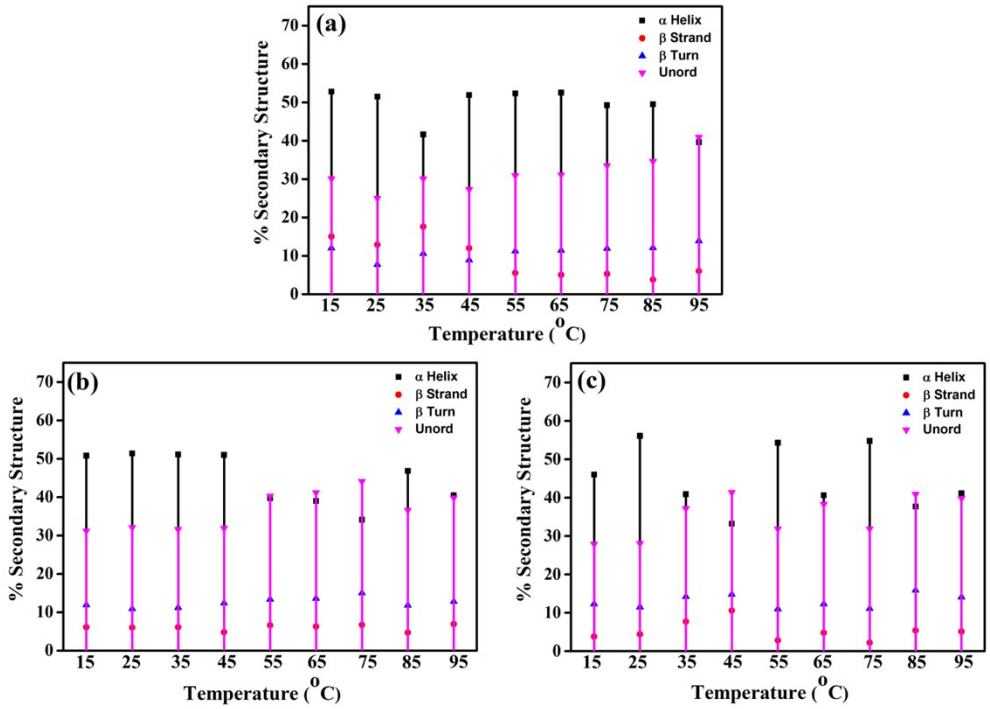

Figure S10. The assessment of secondary structure components of the Cyt-c has been performed in the presence of AuNP-IL4 with concentrations (a) 2 nM, (b) 6 nM, and (c) 10 nM against temperature gradient from 15 to 95 ºC using dichroweb software.

Absorption Spectra Analysis of Cyt-c in the Presence of Different Concentration of AuNP-ILs

As presented in Figure S11 (a), with an increase in concentration from 2 nM to 6 nM of Naked AuNP, the intensity of both the soret band and Q band increased which directs a shift of heme moiety towards a non-polar environment.[32] Further, in presence of all studied concentrations of AuNP-IL1 (Figure S11 (b)), no significant change in absorbance maxima was observed. This observation reveals that the orientations of heme moieties with existing bonds are well preserved. The effect on the Q band of the Cyt-c is mainly due to the surface plasmon resonance (SPR) of the AuNPs. Furthermore, similar results are observed for AuNP- IL2, AuNP-IL3 and AuNP- IL4 which have been provided in Figures 11 (c), (d) and (e), respectively. There is an increase in absorbance intensity of both the soret band and Q band in a concentration-dependent manner of AuNP-ILs. However, there is a shift in wavelength maxima in either of the soret band or Q bands.

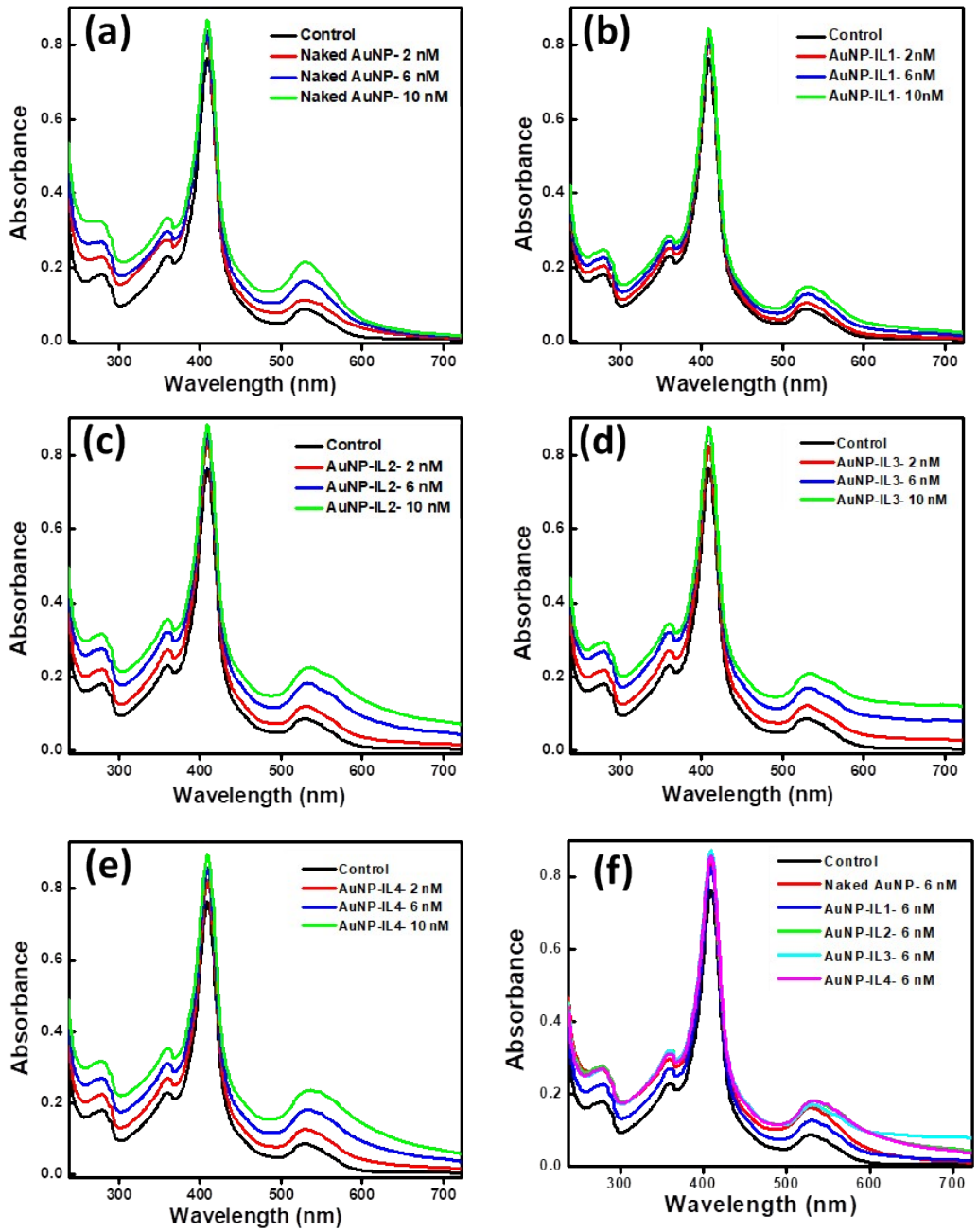

Figure S11. The UV-vis spectral analysis of control Cyt-c (in black) has been represented in the presence of various concentrations of (a) naked AuNP, (b) AuNP-IL1, (c) AuNP-IL2, (d) AuNP-IL3, and (e) AuNP-IL4. Moreover, in Figure f, the variation in the microenvironment of pure Cyt-c has been compared in the presence of all IL-mediated AuNPs at concentration 6 nM.

Table S1. The hydrodynamic diameter, d_H (nm) values of Cyt-c in buffer and in the presence of different IL-mediated AuNPs.

S.No.	Sample	Hydrodynamic Diameter, d_H (nm) values at different concentrations of AuNPs		
		2 nM	**6 nM**	**10 nM**
1.	Pure Cyt-c (0.15 mg/mL)	5.46 ± 0.72		
2.	Naked AuNPs	Peak 1. 39.39 ± 1.86 (88.7%) Peak 2. 406.8 ± 3.61 (10.9%)	Peak 1. 48.27 ± 1.96 (65.4%) Peak 2. 364.8 ± 3.85 (34.6%)	Peak 1. 48.68 ± 1.91 (75.1%) Peak 2. 336.1 ± 2.92 (24.9%)
3.	Cyt-c-AuNPs-IL1	Peak 1. 513.9 ± 4.64 (97.7%)	Peak 1. 526.6 ± 4.96 (97.9%)	Peak 1. 541.5 ± 5.19 (100%)
4.	Cyt-c-AuNPs-IL2	Peak 1. 570.7 ± 5.62 (91.1%) Peak 2. 140.4 ± 2.18 (8.9%)	Peak 1. 665.1± 6.84 (89.6%) Peak 2. 217.4 ± 3.21 (10.4%)	Peak 1. 728.2 ± 8.22 (84.0%) Peak 2. 121.7 ± 1.92 (13.0%)
5.	Cyt-c-AuNPs-IL3	Peak 1. 513.0 ± 4.81 (73.3%) Peak 2. 95.24 ± (26.7%)	Peak 1. 585 ± 6.96 (87.3%) Peak 2. 104.0 ± 2.35 (12.7%)	Peak 1. 667.0 ± 7.22 (100%)
6.	Cyt-c-AuNPs-IL4	Peak 1. 556.9 ± 5.26 (100%)	Peak 1. 563.1 ± 6.39 (74.7%) Peak 2. 71.54 ± 2.53 (25.3%)	Peak 1. 22.84 ± 1.35 (100%)